Sains Malaysiana 53(1)(2024): 149-162
*http://doi.org/10.17576/jsm-2024-5301-12*

# Nonenzymatic Sensor Based on Polythiophene/Titanium Dioxide (PTh/$TiO_2$) Composite for the Determination of Malathion in Water

(Penderia Nonenzim Berdasarkan Komposit Politiofen/Titanium Dioksida (PTh/$TiO_2$) untuk Penentuan Malation dalam Air)

SONGÜL ŞEN GÜRSOY[1,*] & DERYA KAHRAMAN[2]

[1]*Burdur Mehmet Akif Ersoy University, Faculty of Arts and Sciences, Department of Chemistry, TR-15030 Burdur, Turkey*
[2]*Burdur Mehmet Akif Ersoy University, Institute of Applied and Natural Sciences, Department of Chemistry, TR-15030 Burdur, Turkey*

*Received: 7 April 2023/Accepted: 29 December 2023*

ABSTRACT

This study presents a novel nonenzymatic pesticide sensor utilizing a polythiophene/$TiO_2$ (PTh/$TiO_2$) film deposited on a glassy carbon (GC) electrode as the working electrode. The thiophene monomer was polymerized onto $TiO_2$ by cyclic voltammetric method in the range of 0.0-2.5 V with 15 cycles at room temperature. The prepared electrode was used for the sensitive and selective detection of malathion thus providing the basis for facile electrochemical quantification. The surface morphology and crystal structure of the (PTh/$TiO_2$) film were studied by SEM and XRD. FTIR was used for the structural analysis of (PTh/$TiO_2$) film. FTIR results indicated that the PTh/$TiO_2$ composite structure was formed. The smooth surface morphology of PTh/$TiO_2$ was supported by SEM results. XRD analysis verified that PTh is covered on $TiO_2$ particles. The crystal phase of $TiO_2$ was changed to amorph state after PTh modification. Additionally, the electrochemical characterization of polymer film and its response to malathion was examined by the CV method. Under optimized operational conditions, the response of the pesticide sensor was measured by CV in the range of -1 to 2.3 V versus the Ag/AgCl reference electrode due to the electrooxidation of malathion. The analysis focused on current values at -0.73 V, where the reduction of the PTh/TiO2 system occurred upon the addition of known amounts of malathion. The PTh/$TiO_2$ composite film was sensitive to malathion in a linear range from 9.9 ppm to 436 ppm. The sensitivity was calculated as 57.5 µA/ µM $cm^2$ whereas the detection limit was calculated as 7.45 µM. The maximum reaction rate was estimated as 767 µA. The developed sensor also showed good selectivity and reproducibility. The nonenzymatic pesticide sensor was successfully applied to detect malathion in tap water with at least 90% recovery.

Keywords: Conducting polymer; pesticide; polythiophene; $TiO_2$; sensor

ABSTRAK

Kajian ini membentangkan penderia racun perosak nonenzimatik baru yang menggunakan filem politiofen/$TiO_2$ (PTh/$TiO_2$) yang dimendapkan pada elektrod karbon berkaca (GC) sebagai elektrod kerja. Monomer tiofen telah dipolimerkan ke $TiO_2$ melalui kaedah voltametri kitaran dalam julat 0.0-2.5 V dengan 15 kitaran pada suhu bilik. Elektrod yang disediakan telah digunakan untuk pengesanan sensitif dan memilih malation sekali gus menyediakan asas untuk pengkuantitian elektrokimia yang mudah. Morfologi permukaan dan struktur hablur filem (PTh/$TiO_2$) telah dikaji oleh SEM dan XRD. FTIR digunakan untuk analisis struktur filem (PTh/$TiO_2$). Keputusan FTIR menunjukkan bahawa struktur komposit PTh/$TiO_2$ telah terbentuk. Morfologi permukaan licin PTh/$TiO_2$ disokong oleh keputusan SEM. Analisis XRD mengesahkan bahawa PTh diliputi pada zarah $TiO_2$. Fasa kristal $TiO_2$ telah ditukar kepada keadaan amorf selepas pengubahsuaian PTh. Selain itu, pencirian elektrokimia filem polimer dan tindak balasnya terhadap malation telah diperiksa dengan kaedah CV. Di bawah keadaan operasi yang dioptimumkan, tindak balas penderia racun perosak diukur oleh CV dalam julat -1 hingga 2.3 V berbanding elektrod rujukan Ag/AgCl disebabkan

oleh elektrooksidasi malation. Analisis tertumpu pada nilai semasa pada -0.73 V dengan pengurangan sistem PTh/$TiO_2$ berlaku apabila penambahan jumlah malation yang diketahui. Filem komposit PTh/$TiO_2$ adalah sensitif kepada malation dalam julat linear dari 9.9 ppm hingga 436 ppm. Kepekaan dihitung sebagai 57.5 μA/μM $cm^2$ manakala had pengesanan dihitung sebagai 7.45 μM. Kadar tindak balas maksimum dianggarkan sebagai 767 μA. Sensor yang dibangunkan juga menunjukkan keterpilihan dan kebolehulangan yang baik. Penderia racun perosak nonenzim telah berjaya digunakan untuk mengesan malation dalam air paip dengan sekurang-kurangnya 90% pemulihan.

Kata kunci: Penderia; polimer pengalir; politiofen; racun perosak; $TiO_2$

## Introduction

Organophosphorus pesticides (OPs) are a class of organophosphorus compounds used all over the world as insecticides for different kinds of purposes such as in agricultural and medical industries. However, the most characteristic features of these compounds are that they stay in nature for a long time, are toxic and accumulate continuously (Pathak et al. 2022). Wrong and uncontrolled use of pesticides can pose a great threat to human health and the environment such as soil, water and air. For example, heavy use of pesticides damages the immune, nervous and endocrine systems in the body (Mitra et al. 2022). Pesticides are being used widely every day. Therefore, it has become an urgent need to develop new techniques to determine even the smallest amounts in different environments. Malathion is an organophosphate insecticide used in agriculture to remove insects in fruits, vines, vegetables, field crops, and greenhouse crops. Malathion is a neurotoxic insecticide that is quickly penetrated via skin, lungs, mucous membranes or gastrointestinal tract. In addition, it can decrease the acetylcholinesterase activity. As a result, malathion causes symptoms such as unconsciousness and headache (Navarrete-Meneses et al. 2017). $TiO_2$ has been studied a extensively due to its promising properties (electrical, chemical, optical and photoelectric conversion efficiency) in many fields such as photovoltaic devices, electronic cells and sensors (Ebrahimi et al. 2020; Kawagishi, Adachi & Kobayashi 2023; Liu et al. 2023). However, the important thing is to prevent nanoparticles aggregation and improve their dispersibility properties due to the high surface energy. To this end, covering their surfaces with a suitable material will further improve their application areas. For this purpose, conducting polymers could be used to modify the surface of metal oxides. Among conducting polymers, polythiophene is preferred due to its intriguing semiconductor, optical, and electronic properties, along with processing advantages and good mechanical properties (Shirgaonkar et al. 2024). Compared to other conductive polymers it exhibits good stability for practical applications. A large number of different metal oxide particles were used as cores in nanocomposites covered by conductive polymer shells (Nejad, Soleimani-Gorgani & Pishvaei 2023). Polymer-metal oxide composites have been the most frequently studied materials for a long time due to their unique electrical, optical and mechanical properties. The main advantage of these materials is the combination of synergetic and complementary behaviours with composite material (Li & Zhang 2009).

In recent years, conventional analytical techniques such as gas chromatography incorporated with mass spectroscopy, Raman spectroscopy, and acoustic and fluorescence techniques have been used for pesticide determination (Feng et al. 2020; García et al. 2014; Su et al. 2021; Zhang et al. 2021). In fact, these methods are necessary to detect pesticides with high sensitivity and reliability. However, they have disadvantages such as being time-consuming, having preliminary preparation and sample preparation stages, being expensive, having high operating costs, and especially the need for specialized personnel. However, since on-site detection of pesticides in environmental monitoring areas and groundwater may also be required, more useful, direct, rapid and sensitive detection methods are in great demand. Electrochemical techniques are powerful alternatives to traditional methods for determining the trace amounts of pesticides as they have on-site detection, high sensitivity, fast response and economical advantages (Anandhakumar, Dhanalakshmi & Mathiyarasu 2014; Tian et al. 2018; Wang et al. 2014).

Although the determination of pesticides with electrochemical biosensors stands out as a preferred method in recent years, the external conditions such as

temperature, pressure, storage conditions and enzyme activity must be strictly controlled. It is difficult to work with enzyme-based electro-chemical biosensors for pestisite detection. The long preparation phase and analysis time of enzymatic determination have led scientists to seek alternatives in this regard. There are numbers of the studies focused on the electrochemical detection of malathion based on acetylcholinesterase enzyme, AChE, irreversible inhibiton. Some of these AChE based electrochemical biosensors were fabricated using polyaniline–carbon nanotubes (Cesarino et al. 2012), rGO-TEPA-Copper nanowires (Li et al. 2020); $NiCr_2O_4$/g-$C_3N_4$ composite (Bilal et al. 2022), citrate-capped gold nanoparticles (AuNPs)/(3-mercaptopropyl)-trimethoxysilane (MPS)/gold electrode, AuNPs/MPS/Au (Song et al. 2016), and Pt nanoparticles anchored on UiO66-$NH_2$ (Ma et al. 2019).

In recent years, studies for the enzyme-free determination of malathion have become popular. Non-enzymatic methods have proven to be intriguing in the determination of pesticides, offering advantages such as low cost and short analysis time. In non-enzymatic sensor systems, the electrochemical response resulting from the reaction between malathion and the electroactive material on the electrode surface is monitored. In this context, CuO@MWCNTs nanocomposite (Serag et al. 2021), bimetallic Cu-Co metal-organic gels (He et al. 2023), CuO-$CeO_2$ composite (Xie et al. 2019) were used as electroactive substrates. However, it is still essential to investigate new electroactive species for the development of cheap, fast and simple non-enzymatic pesticide sensors.

In this study, we focused on integrating the properties of polythiophene and $TiO_2$ as a transducer to develop a non-enzymatic electrochemical sensor for malathion detection. The developed sensor showed an acceptable detection limit and a wide linear range. The non-enzymatic sensor system was simple, rapid and cheap. The PTh/$TiO_2$-based non-enzymatic malathion sensor was successfully employed for the detection of malathion in tap water.

## Materials and Methods

### Chemicals

Thiophene (Aldrich) was purified by distillation at reduced pressure before use. Tetrabutylammonium hexafluorophosphate ($TBAPF_6$, Sigma), acetonitrile (ACN, Aldrich) and nanodimensional $TiO_2$ (40-50 nm, Aldrich) were used for the synthesis of the composite. $NaH_2PO_4.2H_2O$ (Riedel De Haen) and $Na_2HPO_4.7H_2O$ (Riedel De Haen) were used to prepare the buffer solution. Alumina polishing suspension agglomerate (0.05 cr micron) (Baikowski) was employed to polish the working electrode. Double-distilled water was used for the preparation of the buffer solution. All other compounds were analytical reagent grade.

### Apparatus

The polymer was synthesized by using the electrochemical method with a three-electrode system. Glassy carbon electrode (GCE), Ag/AgCl electrode, and Pt wire were used as working, reference, and auxiliary electrodes, respectively. Polymerization studies and sensor measurements were conducted in three-electrode cells equipped with potentiostat/galvanostat (CompactStat, Ivium Technologies, Netherlands). Indium thin oxide (ITO) electrode was used for the deposition of polymer for FTIR, SEM and X-ray measurements. FTIR spectra were performed between 400 $cm^{-1}$ and 4000 $cm^{-1}$ with a 4 $cm^{-1}$ resolution on a Perkin Elmer Frontier (Beaconsfield, Buckinghamshire, HP91QA, England). For SEM analysis, the JEOL SEM-7100-EDX (Zaventem, Belgium) model scanning electron microscope was used. The X-ray powder diffraction (XRD) data of the samples were recorded on a Bruker AXS D8 Advance Model, X-Ray powder diffractometer (Germany).

### Synthesis of the PTH/$TiO_2$ Film

Electrosynthesis of the PTh/$TiO_2$ film was performed on the surface of GCE by cyclic voltammetry at ambient conditions. Firstly, the GCE was polished with alumina polishing suspension and washed with ethanol and phosphate buffer solution, respectively. The $TiO_2$ suspension solution was prepared by mixing $TiO_2$ in 5 mL of acetonitrile in the presense 0.0465 g of $TBAPF_6$ under ultrasonic agitation for 10 min, resulting in a homogeneous suspension. Subsequently, 0.12 mmol of thiophene was dissolved in this suspension using an ultrasonic bath for 5 minutes. The monomer was polymerized onto $TiO_2$ by cyclic voltammetric method in the range of 0.0-2.5 V with 15 cycles at room temperature (Sari et al. 2003). After the electrosynthesis of the polymer film, the electrode was washed several times with acetonitrile to remove any remaining monomer (Figure 1).

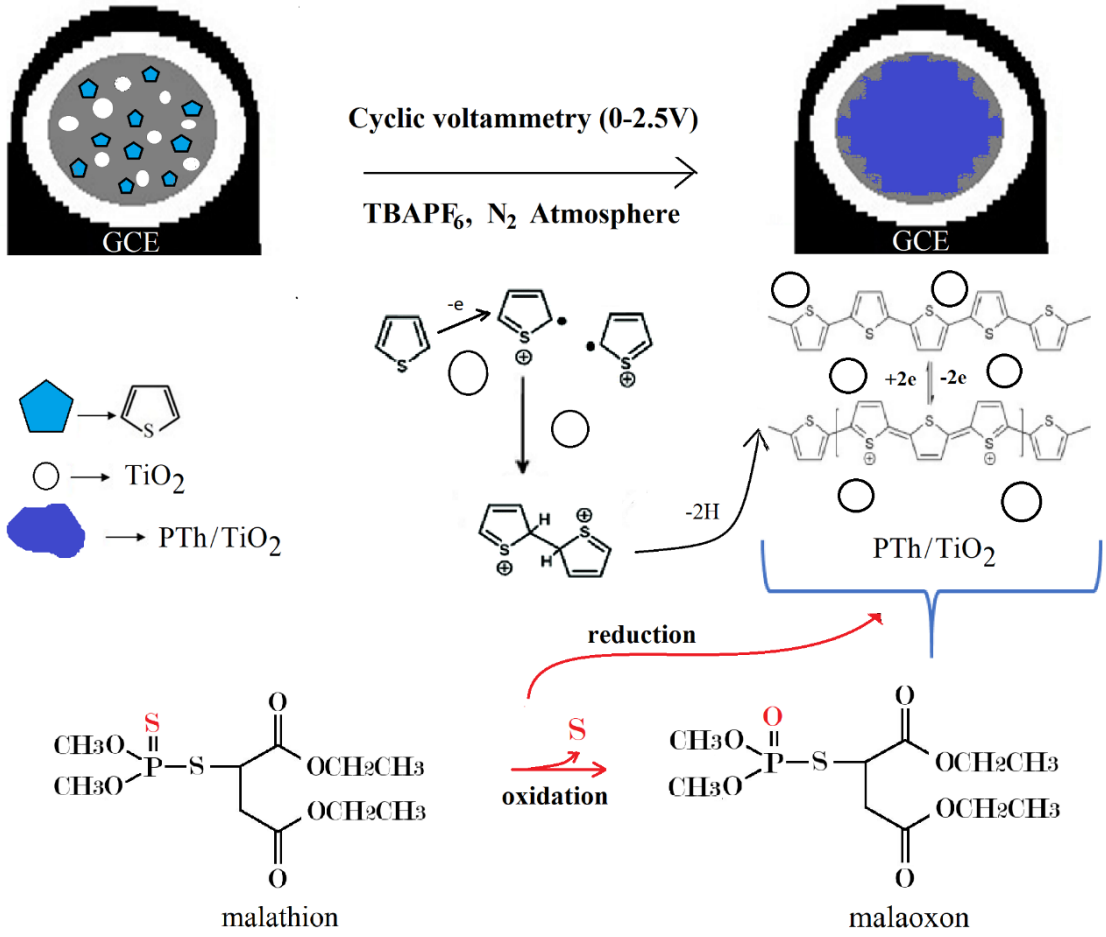


FIGURE 1. Synthesis procedure of $PTh/TiO_2$ composite film and the plausible electrochemical reaction mechanism of malathion at the $PTh/TiO_2$ composite modified GCE

### ESTIMATION OF MALATHION

The electrochemical system and electrodes employed for malathion determination were identical to those utilized in the synthesis of $PTh/TiO_2$. The electrolyte used in the study was 10 mL of 0.1 M $Na_2HPO_4$ buffer solution with an appropriate pH. The response of the $PTh/TiO_2$ film-modified GCE to the malathion was determined in the range of -1 to 2.3 V at a scan rate of 50 mV $s^{-1}$ by the cyclic voltammetry (CV) method. The analysis focused on current values at -0.73 V, where the reduction of the $PTh/TiO_2$ system occurred upon the addition of known concentrations of malathion. Optimization processes, including adjustments to buffer pH and thiophene amount, were carried out for the $PTh/TiO_2$ film-modified working electrode.

## RESULTS AND DISCUSSION

### CYCLIC VOLTAMMETRY (CV)

Figure 2 indicates the cyclic voltammograms of PTh and $PTh/TiO_2$ composite. Additionally, the cyclic voltammogram of $TiO_2$ was monitored in a synthesis solution without thiophene. Experiments were done in unstirred solution onto a GCE disc electrode with 50 mV $s^{-1}$ scan rate between the range of 0-2.5V. PTh could not be accumulated electrochemically under experimental conditions. However, when $TiO_2$ was added to the electrochemical cell before applying the experimental procedure, PTh could be synthesized by covering the surface of $TiO_2$ particles onto the GCE electrode. As

depicted in Figure 2, the onset point of the PTh/$TiO_2$ composite, starting at 1.1 V, aligns with the CV of $TiO_2$. Upon comparing the CVs of the PTh/$TiO_2$ composite and $TiO_2$, it becomes evident that this point extends to 1.3 V in the composite CV. This expansion can be attributed to the polymerization potential of PTh, which is observed at 1.3 V (Fu et al. 2002).

There is a knot seen at about 1V for PTh and PTh/$TiO_2$ composite which is the typical indicator for the electrosynthesis of conducting polymers. The peak at 2.25 V was the main oxidation step of thiophene which is referred to as the doping with $PF_6^-$ (Sari et al. 2003). Based on the electrochemical results, it is evident that the formation of the PTh/$TiO_2$ composite structure was successfully achieved on the glassy carbon electrode (GCE). Following the preparation of the electrosynthesis solution, as described earlier, a cyclic voltammetry experiment was conducted in an unstirred solution with a fixed scan rate of 50 mV $s^{-1}$ for 15 cycles. The onset point of the cyclic voltammogram for polythiophene (PTh) began at 1.2 V. Notably, the electrosynthesis of polythiophene alone is known to be challenging (Sen Gursoy et al. 2020). The $TiO_2$ may play a role both as a nanoparticle to increase the sensitivity of the sensor and as the backdrop to facilitate the electrosynthesis of polythiophene. We used cyclic voltammetry to estimate the quantitative information about a redox system in 0.1 M, pH 6.5 phosphate buffer solution. The scanning rate value between working and reference electrodes has increased each scan cycle. Randles-Sevcik equation explains the peak current at 298 K in a reversible system as provided herewith (Randles 1948; Ševčík 1948):

$$ip = (2.69\times10^5).\ n^{3/2}.A.D^{1/2}.C_o.v^{1/2}$$

where $i_p$ is the peak current (A); n is the number of electrons exchanged during the redox process; D is the diffusion coefficient ($m^2/s$); $C_o$ is the concentration of the analyte ($mol/m^3$); A is the area of the electrode ($m^2$); and v is the experimental scan rate (V/s). This equation describes the influence of scanning rate on peak current in the CV method. In a cyclic voltammetric study, the peak current depends on both the diffusion properties of the electroactive species and the scanning rate (Malanina et al. 2023). Figure 3(a)-3(c) shows the current values versus the scanning rate (25 mV $s^{-1}$ to 225 mV $s^{-1}$) of the PTh/$TiO_2$ film-modified working electrode. Cathodic peak currents which were increased with scanning rate, show that the PTh/$TiO_2$ film is very well attached to the electrode and has excellent stability even after high scanning rates (Figure 3(a)). The findings also supported that the electrochemical process is diffusion-assisted,

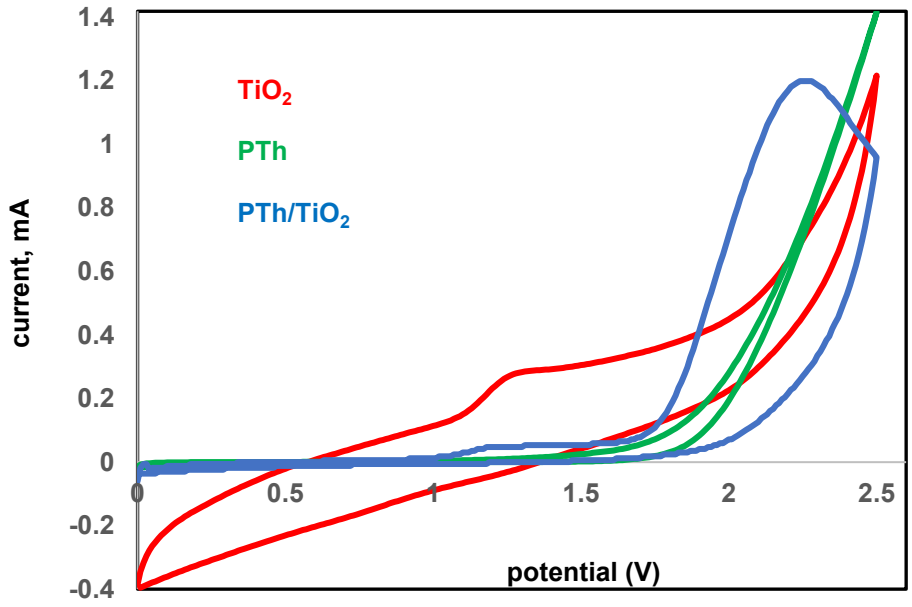


FIGURE 2. Electrochemical synthesis of PTh/$TiO_2$ film (CV, 0-2.5 V, 50 mV $s^{-1}$ scan rate)

given the linearity of the graph (Gursoy et al. 2018) (Figure 3(b)). Additionally, it was observed that the cathodic peak potentials are linear with the logarithm of scan rate at higher scan rates from 100 to 225 $mVs^{-1}$ (Figure 3(c)). These results suggest the quasi-reversible electron transfer system of the composite modified working electrode (Sing et al. 2013).

## FTIR, SEM AND XRD RESULTS

Figure 4(a) shows the FTIR results of $TiO_2$ and PTh/$TiO_2$ composite. Since polythiophene could not be synthesized under the specified conditions, its FTIR spectrum could not be obtained. For comparison, only the FTIR spectra of $TiO_2$ and PTh/$TiO_2$ composite were used. The broad parabolic peak at the range of 3410 $cm^{-1}$ - 3429 $cm^{-1}$ and the band at around 1630 $cm^{-1}$ indicated the presence of OH stretching vibration and the bending vibration of water interacted with $TiO_2$ and PTh/$TiO_2$ due to the moisture in KBr (Senthilkumar, Thenamirtham & Selvan 2011). After preparing the PTh/$TiO_2$ composite, the bands coming from PTh were seen at the FTIR spectrum. Additionally, numerous small peaks indicative of aromatic C–H stretching vibrations for PTh were present at around 3000 $cm^{-1}$. The fingerprint region of PTh was monitored at the range of 600-1500 $cm^{-1}$ (Rahman et al. 2023). The peaks at 1475 $cm^{-1}$ and 1410 $cm^{-1}$ were attributed to C-H stretching and

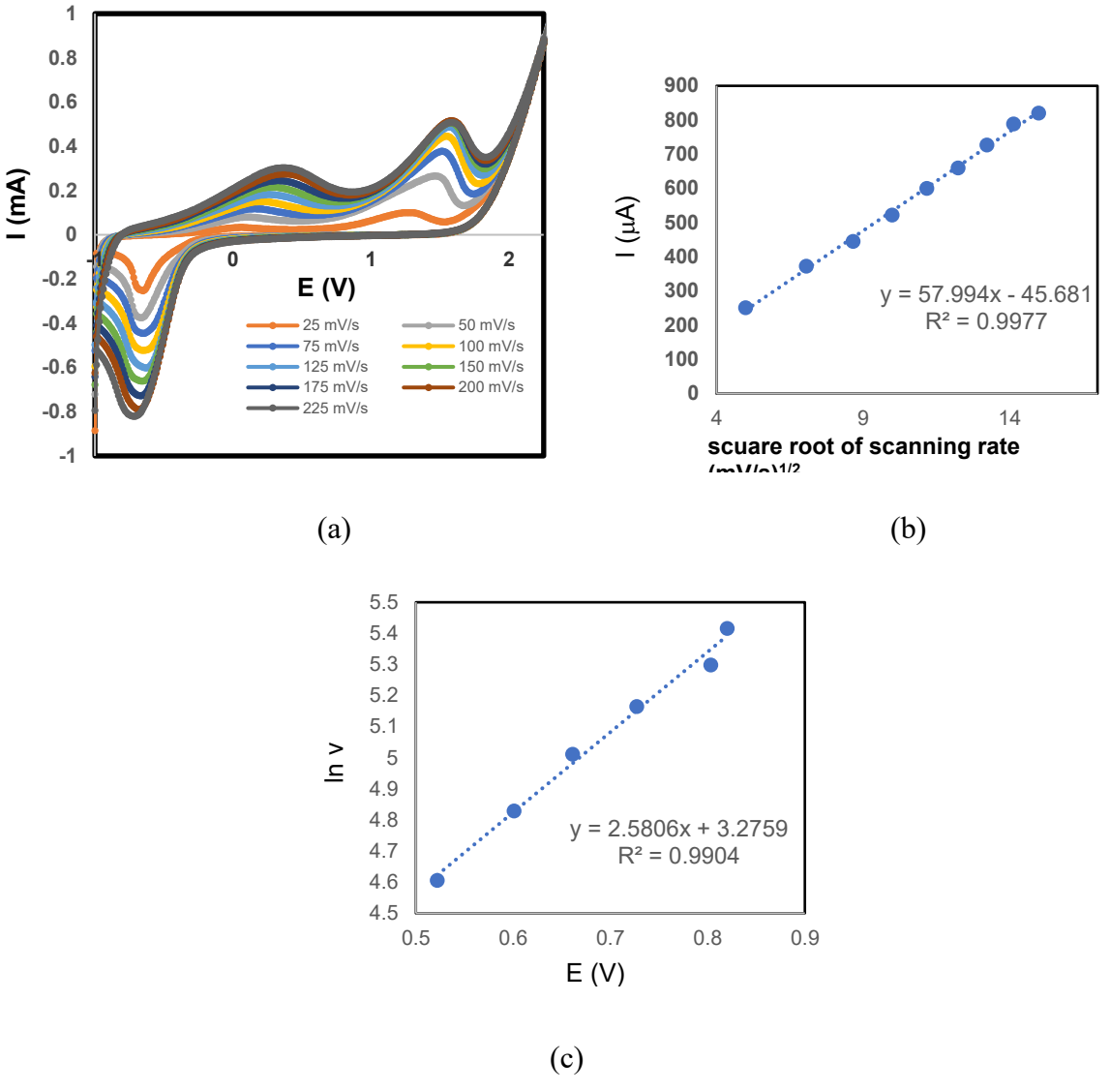


FIGURE 3. The current-potential plots of PTh/$TiO_2$ film-modified GC electrode with different scan rates in the range of 25 mV $s^{-1}$ and 225 mV $s^{-1}$ (a), current versus square root of scan rate ($I\text{-}v^{1/2}$) (b) and potential versus ln of scan rate (100-225 mV $s^{-1}$)(E-ln v) (c)

C=C symmetric stretching of PTh. The peaks at 1220 and 1106 $cm^{-1}$ are generally ascribed to C-H bending and in-plane deformation modes whereas the peak at 740 $cm^{-1}$ is attributed to the C-S bending of PTh. A small bulge peak at 1387 $cm^{-1}$ is attributed to the asymmetric stretching vibration of Ti-O-Ti (Mugundan et al. 2015). The Ti-O stretching vibration is observed clearly at 558 $cm^{-1}$ for the composite structure. These results indicate that the composite was formed by PTh and $TiO_2$.

The formation of the PTh/$TiO_2$ composite structure facilitates the reduction that will occur in the composite structure as a result of the oxidation of malathion. In any case, PTh could not be synthesized electrochemically alone. However, $TiO_2$ nanoparticles has promising properties such as electrical, chemical, optical and photoelectric conversion efficiency. The problem of $TiO_2$ particles coming together to form aggregates was overcome by coating its surface with a conductive polymer such as PTh, which has superior electronic properties, is easily processable and is mechanically durable. Combining these materials together has showed synergistic and complementary behavior. The composite formation supported by FTIR results created a sensitive, selective and stable surface for malathion determination on the GC electrode surface.

SEM images of $TiO_2$ and PTh/$TiO_2$ film were captured to support composite formation and the distinctions between the images were observed. Figure 4(b) and 4(c) refers to the SEM images of $TiO_2$ $TiO_2$ and PTh/$TiO_2$ composite, respectively. The SEM image of the polythiophene could not be used for comparison as it was not collected electrochemically under the specified conditions. $TiO_2$ exhibits characteristic morphology with a large number of particles and very small particle sizes as illustrated in Figure 4(b) (Chang et al. 2014). It is evident that this porous structure is preserved in PTh/$TiO_2$ morphology but the surface has become smoother, more orderly and homogeneous compared to $TiO_2$ (Figure 4(c)). Furthermore, when polythiophene was coated onto the $TiO_2$ surface, the typical homogeneous, cauliflower-like structure of the conducting polymer emerged with uniform $TiO_2$ distribution. The smooth surface morphology ensures that the electron jump event is easy both on the chain and between chains and layers (Gueye et al. 2020). However, composite structure displays a interconnected three-dimensional network microstructure, which can provide an ideal matrix for electron transfer. Such a highly dense network surface structure could provide a large contact area for interaction with malathion and electroactive PTh/$TiO_2$ composite. Thus, the PTh/$TiO_2$ film-modified electrode demonstrates a remarkable electrochemical response to the malathion. In addition, the significant amount of $S^+$ groups of PTh and $TiO_2$ particles interact to form intercrystalline pores. These pores facilitate the diffusion of the analyte which plays an important role in the shape selectivity towards the malathion diffusion.

XRD patterns of $TiO_2$ and PTh/$TiO_2$ were used to support composite film formation and the differences between the images were observed (Figure 4(d), 4(e)). Figure 4(d) illustrates the XRD patterns of $TiO_2$ showing peaks at $2\theta = 25.59°$, 38.33°, 48,41°, 55.33°, and 62.81°, corresponding, respectively, to the (101), (004), (200), (106), and (215) lattice planes of $TiO_2$, indicating signals of the anatase phase (Kwon et al. 2004). The XRD pattern of PTh/$TiO_2$ film exhibits a broad and amorphous diffraction peak at around $2\theta = 20\text{-}30°$. Since PTh displays a homogeneous distribution over $TiO_2$, not all diffraction peaks of $TiO_2$ were observed in the curve. Only the most prominent peak ($2\theta$=25,7°) corresponding to intermolecular p-p stacking was observed in PTh/$TiO_2$ film (Li, Vamvounis & Holdcroft 2002). Although the characteristic PTh broad peak at 25.7° overlaps with the first strong peak of $TiO_2$, the XRD pattern primarily indicates the presence of PTh structure. However, Figure 4(e) indicates differences between the curves of $TiO_2$ and composite film regarding the shape and position of diffraction peaks. This result suggests that polythiophene is covered on $TiO_2$ crystals as a film and the crystal phase of $TiO_2$ was changed by PTh modification. The highly amorphous structure and attractive morphological properties of the PTh/$TiO_2$ composite may have allowed the selective inward diffusion of malathion molecules. The gaps in the amorphous structure may also have increased sensitivity by allowing the passage of a large number of malathion molecules. And also, no apparent impurity diffraction peaks of PTh/$TiO_2$ composites can be observed, indicating that the composites are of high purity. This may have enabled the determination of malathion with high selectivity.

## OPTIMIZATION OF SENSOR

Buffer solutions at different pH were prepared to determine the optimum pH working value of the phosphate buffer solution. The dependence of the electrochemical oxidation of malathion on the pH was studied by cyclic voltammetry in the pH range from 5.5 up to 7.0 plus 100 µL of 1000 ppm malathion addition to

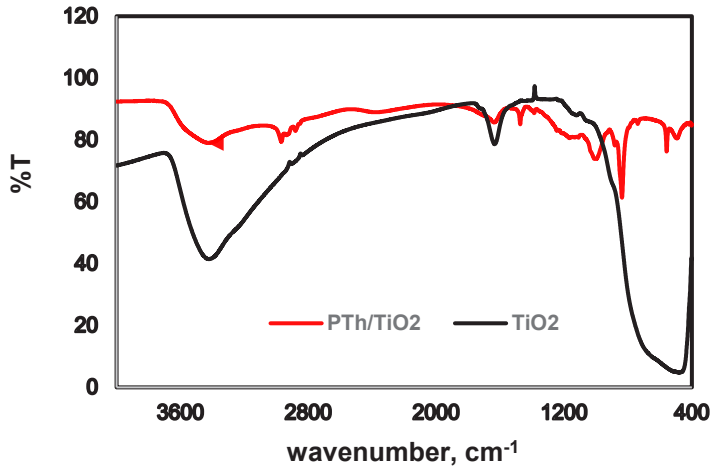


(a)

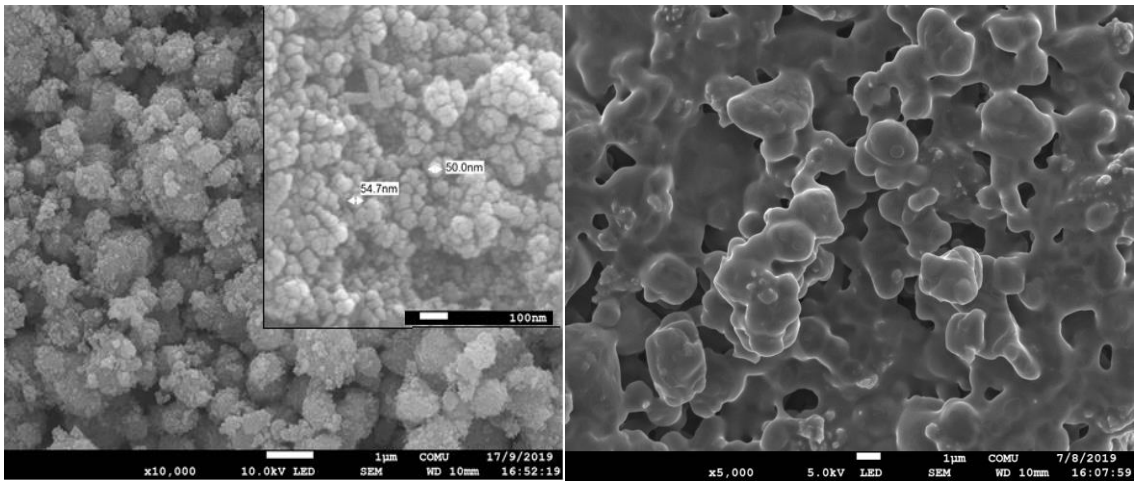


(b) (c)

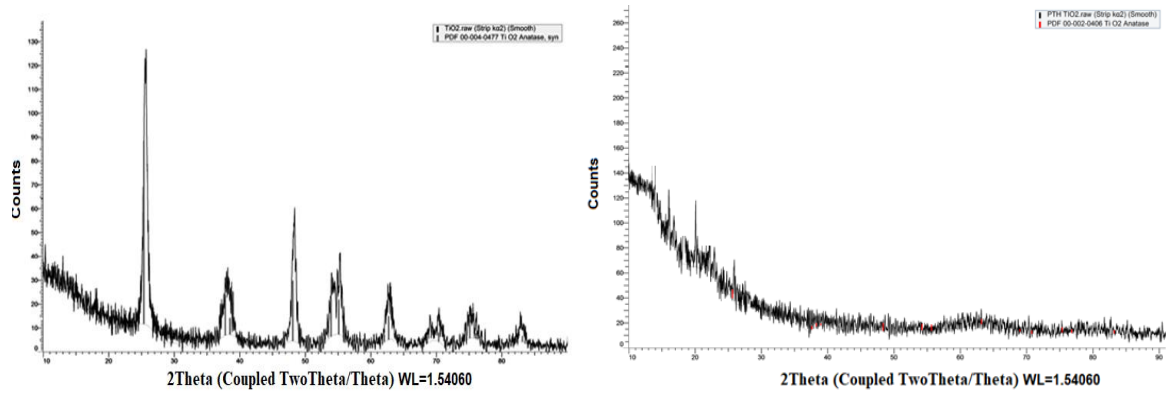


(d) (e)

FIGURE 4. FTIR spectra of $TiO_2$ and $PTh/TiO_2$ (a), SEM images of (b) $TiO_2$, (c) $PTh/TiO_2$, X-Ray spectrum of (d) $TiO_2$ and $PTh/TiO_2$ (e)

the 10 mL buffer solution. Figure 5(a) shows the current values obtained when malathion was added to the buffer solutions with different pHs. As can be seen from the figure, the highest current value was obtained at pH 6.5. Reduction peak potential Ep was observed around -0.73 V vs. Ag/AgCl and the position of the peak did not change significantly with pH variation. However, the intensity of the current was affected by the pH. The adsorption of $H^+$ ions onto the working electrode surface at lower pH values is deposited to potentially inhibit the oxidation mechanism of malathion. Similarly, the degradation of the pesticide structure at higher pH values may have caused a decrease in the electrode performance (Bolat & Abaci 2018). Consequently, pH 6.5 (0.1 M) was selected as the optimal pH value considering the sensitivity for further experiments.

To determine the most suitable composite ratio for malathion determination, the response of the electrode was measured by changing the concentration of thiophene in the synthesis media between 0.012-0.048 M. Since polythiophene does not accumulate on the electrode under these conditions, the effect of polythiophene has not been determined. Among the electrodes modified with composites in different compositions, the composite containing 0.024 M of thiophene gave the highest current value. Figure 5(b) shows the effect of the concentration of thiophene on the malathion response of the sensor.

The reproducibility of the proposed sensor system was evaluated by six different sensors independently prepared under the same conditions during the day (Figure 5(c)). The relative standard deviation of 6.2% defined the stability of electrodes to be remarkable. The results showed that the sensor had good reproducibility. The signals of some species including inorganic ions that can interfere with the response of the electrode have also been studied. The selected species for this study are ions that are commonly found in water namely $Ca^{2+,}$ $Cl^-$, $Br^-$, $K^+$, and $NO_3^-$. The species such as glucose, ascorbic acid and uric acid were also studied to examine the effect of interferences on the response of the proposed electrode. It was determined that the effect of interfering compounds on the relative response is insignificant. The variation in the recorded signal for malathion in the presence of the above-mentioned species indicates the selectivity of the developed nonenzymatic pesticide electrode (<10%) suggesting that there is no significant effect of the interferent on the sensor based on PTh/$TiO_2$ film (Figure 5(d)). As a result, it has been observed that the prepared non-enzymatic malathion sensor is reproducible and selective towards malathion.

## THE RESPONSE OF THE SENSOR TO MALATHION

The PTh/$TiO_2$ film served as a sensing platform for the electrochemical detection of malathion. To achieve this, the cyclic voltammetry (CV) technique was employed, utilizing PTh/$TiO_2$ film-modified electrodes (Figure 6(a), 6(b)). The CV curves presented in Figure 6(a) indicate the increase of the reduction peak, centered at -0.73 V, in the negative direction as the malathion concentration increases. This increase in the peak is associated with the reduction process of the PTh/$TiO_2$ film due to the oxidation of malathion, resulting in the generation of electrons (Migliorini et al. 2020). The current is observed to increase linearly with malathion concentration in the range of 9.9-436 ppm (μg $mL^{-1}$) (Figure 6(b)). Electrode response reaches a constant value at about 436 ppm and there is no significant increase in the current value at higher concentrations. This observation suggests that the polymer film has reached saturation at this concentration of malathion for the prepared electrode under the conditions in the measurement environment. Therefore, in these conditions, diffusion restriction will not be important in electrode activity at higher malathion concentrations.

The sensitivity and detection limit of the sensor calculated from the slope and standard deviation of the calibration plot were 19 μA/ppm $cm^2$ and 2.46 ppm, respectively. The maximum reaction rate was estimated as 767 μA. As a result, the performance of the developed pesticide sensor was comparable with the other results reported in the literature (Barahona et al. 2013; Kushwaha & Shukla 2019).

## REAL SAMPLE ANALYSIS

The PTh/$TiO_2$ modified electrode was also tested for the analysis of the tap water to be evaluated for the presence of malathion in it. This analysis was applied to assess the performance of the sensing platform for detecting pesticides in tap water. The tap water sample was taken from our laboratory in Burdur, Turkey and was used without pretreatment. The malathion concentration could not be detected in the tap water. However, the known concentrations of malathion (10, 20 and 30 ppm) were added to the tap water sample and the percentage recoveries were calculated. The recoveries of malathion were found as 91%, 96% and 93% for 10, 20 and 30 ppm, respectively. The linear regression equation obtained is I(μA)=0.9375[malathion]+0.01 with $R^2$=0.997. These results demonstrate that the developed malathion sensor can be effectively utilized for the detection of malathion in real sample analysis, emphasizing its practical applicability in real water samples.

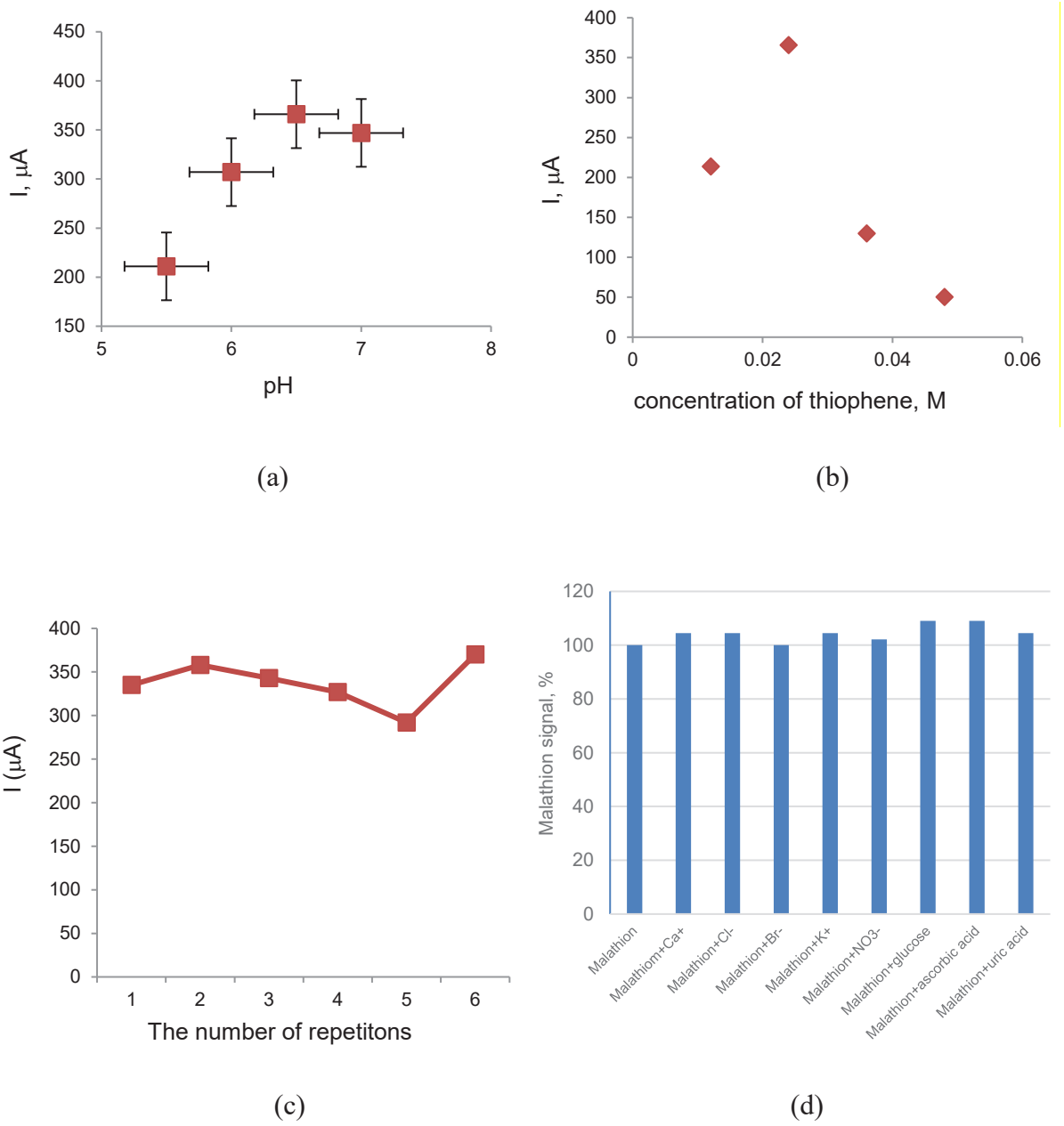


FIGURE 5. Effect of pH on the response of malathion signal of PTh/$TiO_2$ film modified GCE (a), The effect of the concentration of thiophene on the response of the electrode (b), Repeatability (c) and the effect of some interfering species on the response of malathion (d)

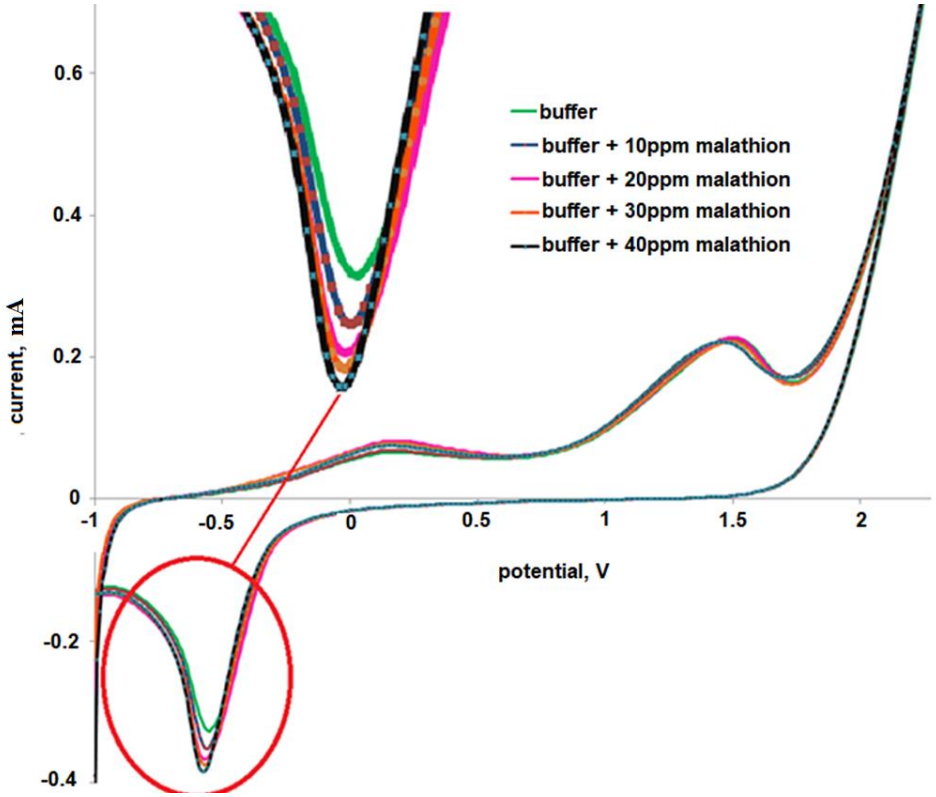


(a)

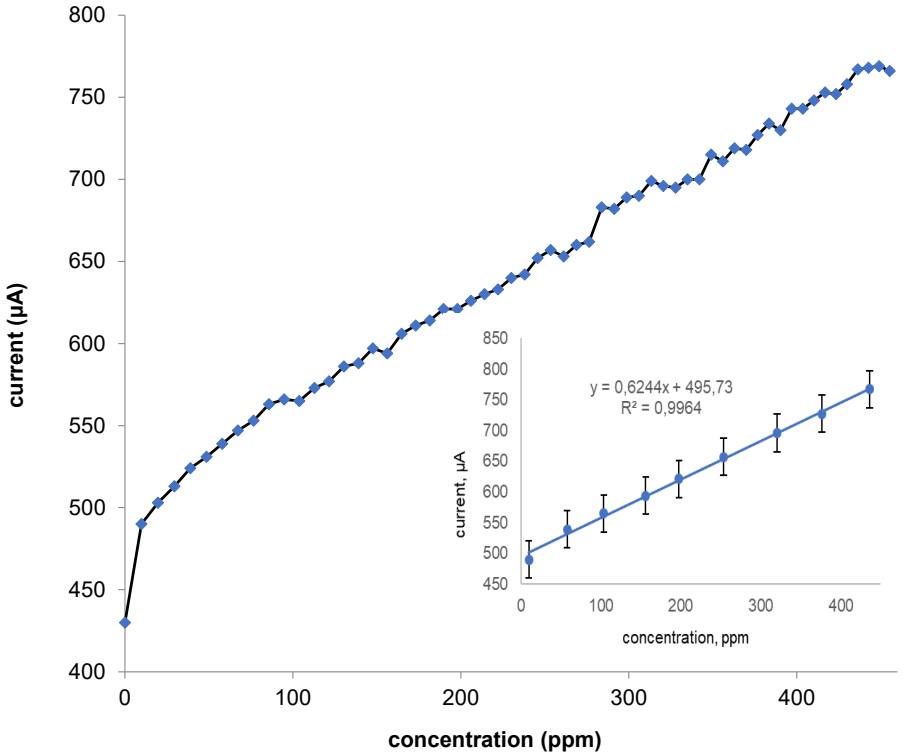


(b)

FIGURE 6. The electrode responses towards the increasing of malathion concentration (a), The effect of malathion concentration on sensor response and linear working range (insider graph) for PTh/$TiO_2$ film modified GCE at -0.73 V in range of -1.0 to 2.3 V applied potential (b)

## Conclusions

In this work, a PTh/$TiO_2$ film-modified carbon paste electrode was developed for the non-enzymatic determination of malathion. The structural and morphological properties and crystal structure of PTh/$TiO_2$ film have been characterized by FTIR, SEM, and XRD analysis, respectively. FTIR results indicated that the composite was formed by PTh and $TiO_2$. SEM results showed the smooth surface morphology of PTh/$TiO_2$ support the electron jump event is easy both on the chain and between chains and layers. XRD analysis suggests that PTh is covered on $TiO_2$ crystals as a film and the crystal phase of $TiO_2$ was changed after PTh modification. Thus, the PTh/$TiO_2$ film-modified electrode demonstrates a remarkable electrochemical response to the malathion. The electrochemical behaviour of PTh/$TiO_2$ film and its response to malathion was examined by cyclic voltammetry. The working conditions were optimized in terms of pH and initial thiophene amount. The optimum pH value was selected as 6.5 considering the sensitivity for further experiments. Among the electrodes modified with composites in different compositions, the composite containing 0,024 M of thiophene gave the highest current value trought malathion concentration. Under optimized conditions, the developed non-enzymatic sensor showed a wide linear range (9.9-436 ppm) and a low detection limit (7.45 µM). The sensitivity was calculated as 57.5 µA/µM $cm^2$ which is comparable value with the literature. The maximum reaction rate was estimated as 767 µA. It also showed good selectivity and reproducibility. The developed sensor was successfully applied to detect of malathion in tap water with high recoveries. The recoveries of malathion were found at least 90% for various addition amounts of malathion. In addition, the results can be evaluated by conducting further studies not only on water analyzes but also on food samples.

## Acknowledgements

The authors thank the Burdur Mehmet Akif Ersoy University, University Scientific Research Projects Commission, and the Department of Chemistry. This work was supported by Burdur Mehmet Akif Ersoy University Scientific Research Projects Commission (Project No: 0407-MP-17). No potential conflict of interest was reported by the authors.

## References

Anandhakumar, S., Dhanalakshmi, K. & Mathiyarasu, J. 2014. Non-enzymatic organophosphorus pesticide detection using gold atomic cluster modified electrode. *Electrochem. Commun.* 38: 15-18.

Barahona, F., Bardliving, C.L., Phifer, A., Bruno, J.G. & Batt, C.A. 2013. An aptasensor based on polymer-gold nanoparticle composite microspheres for the detection of malathion using surface enhanced. Raman spectroscopy. *Ind. Biotechnol.* 9(1): 42-50.

Bilal, S., Nasir, M., Hassan, M.M., Fayyaz ur Rehman, M., Sami, A.J. & Hayat, A. 2022. A novel construct of an electrochemical acetylcholinesterase biosensor for the investigation of malathion sensitivity to three different insect species using a $NiCr_2O_4$/g-$C_3N_4$ composite integrated pencil graphite electrode. *RSC Adv.* 12: 16860-16874.

Bolat, G. & Abaci, S. 2018. Non-enymatic electrochemical sensing of malathion pesticide in tomato and apple samples based on gold nanoparticles-chitosan-ıonic liquid hybrid nanocomposite. *Sensors* 18: 773-789.

Cesarino, I., Moraes, F.C., Lanza, M.R.V. & Machado, S.A.S. 2012. Electrochemical detection of carbamate pesticides in fruit and vegetables with a biosensor based on acetylcholinesterase immobilised on a composite of polyaniline–carbon nanotubes. *Food Chem.* 135: 873-879.

Chang, H.C., Twu, M.J., Hsu, C.Y., Hsu, R.Q. & Kuo, C.G. 2014. Improved performance for dye-sensitized solar cells using a compact $TiO_2$ layer grown by sputtering. *Int. J. Photoenergy* 23: 380120.

Ebrahimi, M., Kermanpur, A., Atapour, M., Adhami, S., Heidari, R.H., Khorshidi, E., Irannejad, N. & Rezaie, B. 2020. Performance enhancement of mesoscopic perovskite solar cells with GQDs-doped $TiO_2$ electron transport layer. *Sol. Energy Mater. and Sol. Cells* 208: 110407.

Feng, C., Xu, Q., Qiu, X., Jin, Y., Ji, J., Lin, Y., Le, S., Wang, G. & Lu, D. 2020. Comprehensive strategy for analysis of pesticide multi-residues in food by GC–MS/MS and UPLC-Q-Orbitrap. *Food Chemistry* 320: 126576.

Fu, M., Shi, G., Chen, F. & Hong, X. 2002. Doping level change of polythiophene film during its electrochemical growth process. *Chem. Chem. Phys.* 4: 2685-2690.

García, J.V., Rocha, M.I., March, C., García, P., Francis, L.A., Montoya, A., Arnau, A. & Jimenez, Y. 2014. Love mode surface acoustic wave and high fundamental frequency quartz crystal microbalance immunosensors for the detection of carbaryl pesticide. *Proc. Eng.* 87: 759-762.

Gueye, M.N., Carella, A., Vincent, J.F., Demadrille, R. & Simonato, J.P. 2020. Progress in understanding structure and transport properties of PEDOT-based materials: A critical review. *Prog. Mater. Sci.* 108: 100616.

Gursoy, O., Sen Gursoy, S., Cogal, S. & Celik Cogal, G. 2018. Development of a new two-enzyme biosensor based on poly(pyrrole-Co-3,4-ethylenedioxythiophene) for lactose determination in milk. *Polym. Eng. Sci.* 58: 839-848.

He, C., Yan, R., Gao, X., Xue, Q. & Wang, H. 2023. Non-enzymatic electrochemical malathion sensor based on bimetallic Cu-Co metal-organic gels modified glassy carbon electrode. *Sensors and Actuators B: Chemical* 385: 133697.

Ji, L. & Zhang, J. 2009. Synthesis, characterization and electrorheological properties of polyaniline/titanate core-shell composite. *Journal of Macromolecular Science, Part A* 7(46): 688-693.

Kawagishi, T., Adachi, Y. & Kobayashi, T. 2023. Photovoltaic performances of $TiO_2$/Se heterojunction devices with different crystallographic structures of sputter-deposited $TiO_2$ thin films. *Materials Chemistry and Physics* 297: 127371.

Kushwaha, C.S. & Shukla, S.K. 2019. Non-enzymatic potentiometric malathion sensing over chitosan-grafted polyaniline hybrid electrode. *J. Mater. Sci.* 54(15): 10846-10855.

Kwon, C.H., Shin, H., Kim, J.H., Choi, W.S. & Yoon, K.H. 2004. Degradation of methylene blue via photocatalysis of titanium dioxide. *Mater. Chem. Phys.* 86(1): 78-82.

Li, Y., Vamvounis, G. & Holdcroft, S. 2002. Tuning optical properties and enhancing solid-state emission of poly(thiophene)s by molecular control: A postfunctionalization approach. *Macromolecules* 35(18): 6900-6906.

Li, S., Qu, L.M., Wang, J.F., Ran, X.Q. & Niu, X. 2020. Acetylcholinesterase based rGO-TEPA-Copper nanowires biosensor for detecting malathion. *International Journal of Electrochemical Science* 15(1): 505-514.

Liu, Y.H., Liu, C., Wang, X.H., Li, T. & Zhang, X. 2023. Electrochemical sensor for sensitive detection of bisphenol A based on molecularly imprinted $TiO_2$ with oxygen vacancy. *Biosensors and Bioelectronics* 237: 115520.

Ma, L., He, Y., Wang, Y., Wang, Y., Li, R., Huang, Z., Jiang, Y. & Gao, J. 2019. Nanocomposites of Pt nanoparticles anchored on UiO66-$NH_2$ as carriers to construct acetylcholinesterase biosensors for organophosphorus pesticide detection. *Electrochimica Acta* 318: 525-533.

Malanina, A., Kuzin, Y., Khadieva, A., Shibaeva, K., Padnya, P., Stoikov, I. & Evtugyn, G. 2023. Voltammetric sensor for doxorubicin determination based on self-assembled DNA-polyphenothiazine composite. *Nanomaterials* 13(16): 2369.

Migliorini, F.L., Sanfelice, R.C., Mercante, L.A., Facure, M.H.M. & Correa, D.S. 2020. Electrochemical sensor based on polyamide 6/polypyrrole electrospun nanofibers coated with reduced graphene oxide for malathion pesticide detection. *Mater. Res. Express* 7: 015601.

Mitra, S., Chakraborty, A.J., Tareq, A.M., Bin Emran, T., Nainu, F., Khusro, A., Idris, A.M., Khandaker, M.U., Osman, H., Alhumaydhi, F.A. & Simal-Gandara, J. 2022. Impact of heavy metals on the environment and human health: Novel therapeutic insights to counter the toxicity. *Journal of King Saud University - Science* 34(3): 101865.

Mugundan, S., Rajamannan, B., Viruthagiri, G., Shanmugam, N., Gobi, R. & Praveen, P. 2015. Synthesis and characterization of undoped and cobalt-doped $TiO_2$ nanoparticles via sol-gel technique. *App. Nanosci.* 5: 449-456.

Navarrete-Meneses, M.P., Salas-Labadía, C., Sanabrais-Jiménez, M., Santana-Hernández, J., Serrano-Cuevas, A., Juárez-Velázquez, R. & Pérez-Vera, P. 2017. Exposure to the insecticides permethrin and malathion induces leukemia and lymphoma-associated gene aberrations *in vitro. Toxicol. In Vitro* 44: 17-26.

Nejad, S.A.T., Soleimani-Gorgani, A. & Pishvaei, M. 2023. Multifunctional screen-printed films using polymer nanocomposite based on PPy/$TiO_2$: Conductive, photocatalytic, self-cleaning and antibacterial functionalities. *Iran Polym. J.* 32: 647-659.

Rahman, S., Rahman Khan, M.M., Deb, B., Dana, S.I. & Ahmed, M.K. 2023. Effective and simple fabrication of pyrrole and thiophene-based poly (Py-co-Th)/ZnO composites for high photocatalytic performance. *South African Journal of Chemical Engineering* 43: 303-311.

Randles, J.E.B. 1948. A cathode ray polarograph. Part II. The current-voltage curves. *Trans. Faraday Soc.* 44: 327-338.

Sari, B., Talu, M., Yildirim, F. & Balci, E.K. 2003. Synthesis and characterization of polyurethane/polythiophene conducting copolymer by electrochemical method. *Appl. Surf. Sci.* 205: 27-38.

Sen Gursoy, S., Yildiz, A., Celik Cogal, G. & Gursoy, O. 2020. A novel lactose biosensor based on electrochemically synthesized 3,4-ethylenedioxythiophene/thiophene (EDOT/Th) copolymer. *Open Chem.* 18: 974-985.

Senthilkumar, B., Thenamirtham, P. & Selvan, R.K. 2011. Structural and electrochemical properties of polythiophene. *Appl. Surf. Sci.* 257: 9063-9067.

Serag, E., El-Maghraby, A., Hassan, N. & El Nemra, A. 2021. CuO@MWCNTs nanocomposite as non-enzyme electrochemical sensor for the detection of Malathion in seawater. *Desalination and Water Treatment* 236: 240-249.

Ševčík, A. 1948. Oscillographic polarography with periodical triangular voltage. *Collect Czech Chem. Commun.* 13: 349-377.

Shirgaonkar, D.B., Yewale, M.A., Shin, D.K., Pawar, S.D., Gunjakar, J.L., Mathad, S.N., Deokate, R.J. & Nakate, U.T. 2024. Nanofibrous polythiophene-$SnO_2$ composite films: A novel approach for low-temperature $NO_2$ sensing. *Materials Science and Engineering: B* 299: 116959.

Sing, A., Sinsinbar, G., Choudhary, M., Kumar, V., Pasricha, R., Verma, H.N., Singh, S.P. & Arora, K. 2013. Graphene oxide-chitosan nanocomposite based electrochemical DNA biosensor for detection of typhoid. *Sens. Actuators B Chem.* 185: 675-684.

Song, Y., Chen, J., Sun, M., Gong, C., Shen, Y., Song, Y. & Wang, L. 2016. A simple electrochemical biosensor based on AuNPs/MPS/Au electrode sensing layer for monitoring carbamate pesticides in real samples. *J. Hazard Mater.* 304: 103-109.

Su, D., Li, H., Yan, Xu., Lin, Y. & Lu, G. 2021. Biosensors based on fluorescence carbon nanomaterials for detection of pesticides. *TrAC Trends in Analytical Chemistry* 134: 116126.

Pathak, V.M., Verma, V.K., Rawat, B.S., Kaur, B., Babu, N., Sharma, A., Dewali, S., Yadav, M., Kumari, R., Singh, S., Mohapatra, A., Pandey, V., Rana, N. & Maria, J. 2022. Current status of pesticide effects on environment, human health and it's eco-friendly management as bioremediation: A comprehensive review. *Front Microbiol.* 13: 962619.

Tian, X., Liu, L., Li, Y., Yang, C., Zhou, Z., Nie, Y. & Wang, Y. 2018. Nonenzymatic electrochemical sensor based on CuO-$TiO_2$ for sensitive and selective detection of methyl parathion pesticide in ground water. *Sensors and Actuators B: Chemical* 256: 135-142.

Wang, M., Huang, J., Wang, M., Zhang, D. & Chen, J. 2014. Electrochemical nonenzymatic sensor based on CoO decorated reduced graphene oxide for the simultaneous determination of carbofuran and carbaryl in fruits and vegetables. *Food Chem.* 151: 191-197.

Xie, Y., Tu, X., Ma, X., Fang, Q., Liu, G., Dai, R., Qu, F., Yu, Y., Lu, L. & Huang, X. 2019. A CuO-$CeO_2$ composite prepared by calcination of a bimetallic metal-organic framework for use in an enzyme-free electrochemical inhibition assay for malathion. *Microchim. Acta* 186: 567.

Zhang, D., Liang, P., Chen, W., Tang, Z., Li, C., Xiao, K., Jin, S., Ni, D. & Yu, Z. 2021. Rapid field trace detection of pesticide residue in food based on surface-enhanced Raman spectroscopy. *Microchim. Acta* 188: 370.

*Corresponding author; email: ssen@mehmetakif.edu.tr